

Fermi surface reconstruction at optimum doping in high- T_c superconductors

F. F. Balakirev^{1*}, J. B. Betts¹, A. Migliori¹, I. Tsukada², Yoichi Ando³, G. S. Boebinger⁴

¹ *National High Magnetic Field Laboratory, Los Alamos National Laboratory, Los Alamos, NM 87545, USA.*

² *Central Research Institute of Electric Power Industry, Komae, Tokyo 201-8511, Japan.*

³ *Institute of Scientific and Industrial Research, Osaka University, 8-1 Mihogaoka, Ibaraki, Osaka 567-0047, Japan*

⁴ *National High Magnetic Field Laboratory and Florida State University, Tallahassee, FL 32310, USA.*

**e-mail:fedor@lanl.gov*

The phenomenon of high temperature superconductivity (HTS) occurs in the transition region between an undoped Mott insulator and a Fermi-liquid-like metal with a large Fermi surface¹. Many theorists speculate that HTS results from the proximity of a quantum phase transition (QPT) in the underlying normal state²⁻⁵. The existence, location and nature of such a QPT have long been obscured by the superconducting phase; however, normal state behavior at low temperatures emerges once the HTS phase is suppressed with intense magnetic fields⁶⁻⁷. Here we show an anomalous peak in the Hall number that is located precisely at optimum doping in two different hole-doped HTS systems. The peak onset is ascribed to the emergence of *electron* pockets. The peak is destroyed due to the loss of Brillouin zone folding when the pseudogap collapses. These observations provide direct evidence of a Fermi surface reconstruction associated with a QPT near optimum doping.

With initial doping of the parent Mott insulator, even the question of whether the charge carriers form conventional Fermi pockets remains controversial. Angle-resolved photoemission spectroscopy (ARPES) finds well-defined quasiparticles, first near the $(\pi/2, \pi/2)$ point in the Brillouin zone, then with further doping, extending along an arc that is roughly tracing the perimeter of a circle centered on (π, π) ^{8,9}. Debate centers on whether ARPES somehow ‘misses’ a piece of the Fermi surface, which is proposed to form a ‘small pocket’ of carriers. Recent magneto-transport measurements using pulsed magnetic fields as high as 85 tesla have found quantum oscillations in two different

underdoped compounds of yttrium-barium-copper-oxide, Ortho-II ordered $\text{YBa}_2\text{Cu}_3\text{O}_{6.5}$ ¹⁰ and $\text{YBa}_2\text{Cu}_4\text{O}_8$ ^{11,12} with effective Cu-O plane doping of 0.10 and 0.12 respectively. These oscillations exhibit the behavior of the well-known Shubnikov-deHaas (SdH) oscillations and thus provide strong evidence of a small and conventional Fermi surface pocket in underdoped cuprates, although its shape and location in the Brillouin zone is still unknown.

In the overdoped regime, detailed angular magneto-resistance oscillations (AMRO) measurements, using a 45T DC magnetic field and a two-axis sample tilt stage have provided a complete mapping of the Fermi surface for the single layer thallium cuprate, $\text{Tl}_2\text{Ba}_2\text{CuO}_{6+\delta}$. They reveal a corrugated cylindrical Fermi surface, consistent with the largely two-dimensional nature of the cuprates that describes a large pocket of carriers centered on (π, π) ¹. The central questions remain: (a) how the evidence of these two distinct states can be reconciled, and (b) can it provide a framework in which to understand both high-temperature superconductivity and the complex phase diagram of the HTS cuprates. Indeed, a number of HTS models are based on the concept that anomalous electronic properties, including the linear temperature dependence of the resistivity, are governed by the existence of a quantum critical point (QCP). Such a QCP is thought to arise from competition between different and still-uncharacterized ground states. Because fluctuations near a critical point can mediate pairing between quasiparticles, quantum fluctuations are conjectured to account for HTS itself. Universal scaling behavior reported in neutron scattering¹³, ARPES¹⁴, and infrared spectroscopy¹⁵ is considered as evidence of criticality. The goal of our transport measurements in high

magnetic fields is to determine the existence and nature of an underlying QPT, as well as its location in the phase diagram, by studying the behavior of the normal state in the low-temperature limit.

Extremely intense magnetic fields are required to destroy the superconducting state in the cuprate superconductors to reveal the resistive normal state well below the superconducting transition temperature, T_c . In this state, longitudinal resistivity, ρ_{ab} , exhibits minimal variation with magnetic field while Hall resistivity, ρ_{Hall} , is roughly linear with magnetic field. Both display dramatic changes as a function of doping.

Figure 1 shows the magnetic field dependence of ρ_{Hall} in superconducting $\text{La}_{2-p}\text{Sr}_p\text{CuO}_4$ (LSCO) thin films and the magnetic field dependence of the Hall coefficient, $R_H = \rho_{Hall}(H)/H$, for the samples at 20K (see Methods and supplementary information for details). The magnetic field dependence of R_H (Fig. 1b) has two dominant attributes: (a) there is no evidence of a magnetic field induced phase transition or sharp change in the number of carriers. That is, the suppression of superconductivity with magnetic field seems to reveal the normal state transport, and (b) R_H in the normal state generally becomes smaller as the Sr doping, p , is increased. This is expected behavior for a simple single band metal, in which the number of charge carriers is inversely proportional to the magnitude of R_H . The most striking feature of Fig. 1b, however, is that R_H is *not a strictly monotonic function of doping* at doping ranges near $p \sim 0.17$.

Figure 2 displays the temperature dependence of the high-field R_H extracted from the high-field Hall resistivity measurements (dashed lines in Fig. 1a, which are constrained to

extrapolate to zero at $H=0$). We note that R_H is monotonic at high temperatures, but below 50K several $R_H(T)$ curves cross. Figure 2b magnifies the complete data set near optimum doping, evidencing a clear local minimum in the doping dependence for R_H at low temperatures at $p=0.175$.

Figure 3a shows the temperature and doping dependence of $1/R_H$ in the normal state of LSCO. Throughout this paper, we plot $1/R_H$ normalized to the number of holes per copper atom and refer to it as the “Hall number”. Of course, in the cuprates this might not be the correct interpretation; however, this expression should be applicable at least for small p ¹⁶. Furthermore, it remains quantitatively precise for all p and provides distinct advantages in communicating the magnitude of $1/R_H$ in familiar units.

The salient feature of the low temperature Hall number is the peak that develops near $p=0.175$ at temperatures below ~ 30 K. The peak appears on the background of the otherwise monotonic increase of Hall number with increased doping. This peak is not unique to LSCO – a strikingly similar feature is seen in another superconducting cuprate, single-layer $\text{Bi}_2\text{Sr}_{2-x}\text{La}_x\text{CuO}_{6+\delta}$ (BSLCO)⁶ (Fig. 3b). The peak in each compound: (a) occurs precisely at optimum doping, which we define as the doping corresponding to the highest value of T_c *in this same set of samples*; (b) exhibits a narrow width of $\delta p \sim \pm 0.01$; (c) is largely obscured at zero magnetic fields by the presence of the superconducting phase, i.e. it emerges only below a threshold temperature approximately equal to the maximum value of T_c ; (d) appears to have a peak value slightly above one carrier per copper atom.

It is not known if the peak in the Hall number can be quantitatively interpreted as a precise value for the number of carriers, as this interpretation implies a simple single band metal with an isotropic quasiparticle scattering rate around the Fermi surface. We will argue, however, that the peak in the Hall number of both LSCO and BSLCO directly evidences a particular topological change in the normal state Fermi surface near optimum doping as the cuprates evolve from a small carrier density (p) metal to a large $(1+p)$ carrier density metal .

The apparent existence of Fermi surfaces in both the underdoped and overdoped regime motivates a description of our Fig. 3 data using the simplest Fermi-surface-based evolution (Figure 4) that can qualitatively account for the observed non-monotonic doping dependence of the Hall number. In the overdoped regime, the Hall data are consistent with large pockets in the Brillouin zone¹ (Fig. 4c). In the underdoped regime, the Hall data are consistent with hole-like quasiparticles located near $(\pi/2, \pi/2)$ in the Brillouin zone^{8,9} (Fig. 4a) resulting from zone folding due to a modulation vector $Q \sim (\pi, \pi)$. The antiferromagnetic modulation vector $Q = (\pi, \pi)$ in the undoped ($p = 0$, half-filled) cuprate and vestiges of this modulation are retained upon hole doping: neutron scattering finds strong spin correlations with an incommensurate modulation vector near $Q \sim (\pi, \pi)$ in the pseudogap regime^{17,18}. Transport measurements could reflect the effects of a $Q \sim (\pi, \pi)$ modulation (Figs. 4a and 4b) even if the modulation is somewhat incommensurate,

fluctuating or short-range, so long as the time and length scales of the modulation are longer than the quasiparticle life time and mean free path.

The crossover from small to large Fermi surface would result from the loss of the (π, π) modulations of the pseudogap regime. Extrapolations of NMR, specific heat and resistivity data taken above T_c suggest the collapse of the pseudogap phase at $p \sim 0.19$ ¹⁹. Indeed, muon spin relaxation and ac susceptibility suggest that the magnetism in LSCO weakens with increased doping and does not vanish until the vicinity of optimum doping²⁰. A number of theoretical approaches also extend the (π, π) modulation toward optimum doping, including antiferromagnetic correlations²¹, the d -density wave²² and staggered flux phase²³ scenarios with prediction of small Fermi pocket formation^{24,25}. These experiments and analyses rely on measurements above T_c or on samples *that are still superconducting*. Only intense magnetic fields provide direct experimental access to the low-temperature normal state near optimum doping.

Simple loss of modulation, leading directly from the Fermi surface topology in Fig. 4a to that in Fig. 4c cannot give a non-monotonic behavior of the Hall number. There is, however, a natural explanation for the existence of a local peak in Hall number upon collapse of the pseudogap state. In Fig. 4a, the pseudogap state has a large energy gap at $(\pm\pi, 0)$ and $(0, \pm\pi)$, hence no carrier pockets centered on those points. As the pseudogap energy scale decreases with doping, electron pockets centered on these points (Fig. 4b) can emerge as a result of zone folding. Because these are electron-like pockets, the sign of their contribution to the Hall effect is opposite to that of the hole quasiparticles near

$(\pi/2, \pi/2)$, reducing the net Hall effect signal (and increasing the Hall number) at low temperatures, as occurs in a compensated semi-metal. The increase in Hall number at low temperatures will be observed if the electron mobility is substantially bigger than the mobility of the holes to compensate for the smaller size of the electron pockets. At high temperatures the difference in the mobility of the two carriers diminish due to thermal broadening and Hall effect is dominated by the bigger hole pockets. Upon further doping, the electron pockets will necessarily be destroyed by the loss of the (π, π) modulation upon collapse of the pseudogap state, occurring at the same doping at which the large hole pocket around (π, π) emerges (Fig. 4c).

The evolution of the Fermi surface in Fig. 4 is very similar to the reported reconstruction of the Fermi surface in an electron-doped cuprate superconductor across the antiferromagnetic transition²⁶, in which doping with *electrons* first forms electron pockets at $(\pm\pi, 0)$ and $(0, \pm\pi)$, followed by the appearance of a hole quasiparticles around $(\pi/2, \pi/2)$. Upon further doping, the electron and hole pockets recombine to form a single, large Fermi pocket.

Observation of the same phenomena in the Hall number of two different hole-doped HTS systems suggests a common quantum phase transition underlying the high-temperature superconducting dome. The peak in the Hall number at optimum doping is interpreted as the precursor of the collapse of the pseudogap state. Critical behavior in the vicinity of a quantum phase transition has long been conjectured as a framework in which to

understand both high-temperature superconductivity and the complex phase diagram of the HTS cuprates²⁻⁵. Criticality has been linked to the well-known linear temperature dependence of the resistivity for all cuprates at optimum doping as well as the nucleation of singular, attractive quasiparticle interactions in the doped antiferromagnetic state². The Hall data offer a first detailed evidence for a phase transition that could be responsible for these critical fluctuations.

Methods

The LSCO thin-film samples studied here were prepared by laser ablation using strontium titanate (STO) substrates²⁷ with eleven values of Sr doping p from 0.08 to 0.22 ($p=0.08, 0.12, 0.14, 0.16, 0.165, 0.17, 0.175, 0.18, 0.19, 0.20$, and 0.22). All films were characterized by X-ray diffraction and uniformity of low-field magnetotransport properties. All samples show metallic behavior for in-plane transport (i.e. $d\rho_{ab}/dT > 0$) at all temperatures above the superconducting transition temperature, T_c . The samples were patterned in a conventional Hall bar geometry for simultaneous measurement of the longitudinal resistivity (ρ_{ab}) and Hall resistivity (ρ_{Hall}). The high magnetic field measurements were performed at National High Magnetic Field Laboratory where a 50 T to 65 T magnetic field was applied perpendicular to the films.

References and Notes

1. Hussey, N. E., Abdel-Jawad, M., Carrington, A., Mackenzie, A. P. & Balicas, L. Observation of a coherent three-dimensional Fermi surface in a high-transition temperature superconductor. *Nature* **425**, 814-817 (2003).

2. Sachdev, S. & Ye, J. Universal quantum-critical dynamics of two-dimensional antiferromagnets. *Phys. Rev. Lett.* **69**, 2411-2414 (1992).
3. Perali, A., Castellani, C., Di Castro, C. & Grilli, M. *d*-wave superconductivity near charge instabilities. *Phys. Rev. B* **54**, 16216–16225 (1996).
4. Varma, C. Pseudogap phase and the quantum-critical point in copper-oxide metals. *Phys. Rev. Lett.* **83**, 3538-3541 (1999).
5. Kivelson, S. A., Fradkin, E. & Emery, V. J. Electronic liquid-crystal phases of a doped Mott insulator. *Nature* **393**, 550–553 (1998).
6. Balakirev, F. F. *et al.* Signature of optimal doping in Hall-effect measurements on a high-temperature superconductor. *Nature* **424**, 912-915 (2003).
7. Dagan, Y., Qazilbash, M. M., Hill, C. P., Kulkarni, V. N. & Greene, R. L. Evidence for a quantum phase transition in $\text{Pr}_{2-x}\text{Ce}_x\text{CuO}_{4+\delta}$ from transport measurements. *Phys. Rev. Lett.* **92**, 167001 (2004).
8. Norman, M. R. *et al.* Destruction of the Fermi surface in underdoped high- T_c superconductors. *Nature* **392**, 157-160 (1998).
9. Yoshida, T. *et al.* Metallic behavior of lightly doped $\text{La}_{2-x}\text{Sr}_x\text{CuO}_4$ with a Fermi surface forming an arc. *Phys. Rev. Lett.* **91**, 027001 (2003).
10. Doiron-Leyraud, N. *et al.* Quantum oscillations and the Fermi surface in an underdoped high- T_c superconductor. *Nature* **447**, 565-568 (2007).
11. Yelland, E. A. *et al.* Quantum oscillations in the underdoped cuprate $\text{YBa}_2\text{Cu}_4\text{O}_8$. arXiv:0707.0057.
12. Bangura, A. F. *et al.* Shubnikov-de Haas oscillations in $\text{YBa}_2\text{Cu}_4\text{O}_8$. arXiv:0707.4461.

13. Aepli, G., Mason, T. E., Hayden, S. M., Mook, H. A. & Kulda, J. Nearly singular magnetic fluctuations in the normal state of a high- T_c cuprate superconductor. *Science* **278**, 1432-1435 (1997).
14. Valla, T. *et al.* Evidence for quantum critical behavior in the optimally doped cuprate $\text{Bi}_2\text{Sr}_2\text{CaCu}_2\text{O}_{8+\delta}$. *Science* **285**, 2110-2113 (1999).
15. van der Marel, D. *et al.* Quantum critical behaviour in a high- T_c superconductor. *Nature* **425**, 271-274 (2003).
16. Ando, Y. *et al.* Evolution of the Hall coefficient and the peculiar electronic structure of the cuprate superconductors. *Phys. Rev. Lett.* **92**, 197001 (2004).
17. Lake, B. *et al.* Antiferromagnetic order induced by an applied magnetic field in a high-temperature superconductor. *Nature* **415**, 299-302 (2002).
18. Christensen, N. B. *et al.*, Dispersive excitations in the high-temperature superconductor $\text{La}_{2-x}\text{Sr}_x\text{CuO}_4$. *Phys. Rev. Lett.* **93**, 147002 (2004).
19. Tallon, J. L. & Loram, J. W. The doping dependence of T^* -what is the real high- T_c phase diagram? *Physica C* **349**, 53-68 (2001).
20. Panagopoulos, C. *et al.* Evidence for a generic quantum transition in high- T_c cuprates. *Phys. Rev. B* **66**, 064501 (2002).
21. Oles, A. M. & Zaanen, J. Mean-field theories of the two-band model and the magnetism in high- T_c oxides. *Phys. Rev. B* **39**, 9175-9191 (1989).
22. Chakravarty, S., Laughlin, R. B., Morr, D. K. & Nayak, C. Hidden order in the cuprates. *Phys. Rev. B* **63**, 094503 (2001).
23. Hsu, T. C., Marston, J. B. & Affleck, I. Two observable features of the staggered-flux phase at nonzero doping. *Phys. Rev. B* **43**, 2866-2877 (1991).

24. Lee, P. A. & Wen, X.-G. Vortex structure in underdoped cuprates. *Phys. Rev. B* **63**, 224517 (2001).
25. Chakravarty, S. & Kee, H.-Y. Fermi pockets and quantum oscillations of the Hall coefficient in high temperature superconductors. arXiv: 0710.0608.
26. Armitage, N. P. *et al.* Doping dependence of an *n*-type cuprate superconductor investigated by angle-resolved photoemission spectroscopy. *Phys. Rev. Lett.* **88**, 257001 (2002).
27. Tsukada, I. & Ono, S. Negative Hall coefficients of heavily overdoped $\text{La}_{2-x}\text{Sr}_x\text{CuO}_4$. *Phys. Rev. B* **74**, 134508 (2006).
28. Hwang, H. Y. *et al.* Scaling of the temperature dependent Hall effect in $\text{La}_{2-x}\text{Sr}_x\text{CuO}_4$. *Phys. Rev. Lett.* **72**, 2636-2639 (1994).
29. Millis, A. J. & Norman, M. R. Antiphase stripe order as the origin of electron pockets observed in 1/8-hole-doped cuprates. arXiv: 0709.0106.

Acknowledgments: The work at the National High Magnetic Field Laboratory was supported by the National Science Foundation and DOE Office of Science. YA was supported by KAKENHI 16340112 and 19674002. We thank N. Harrison, P. Lee, and P. Littlewood for discussions.

Author Information: The authors declare no competing financial interests.

Correspondence and requests for materials should be addressed to F.F.B.

(fedor@lanl.gov).

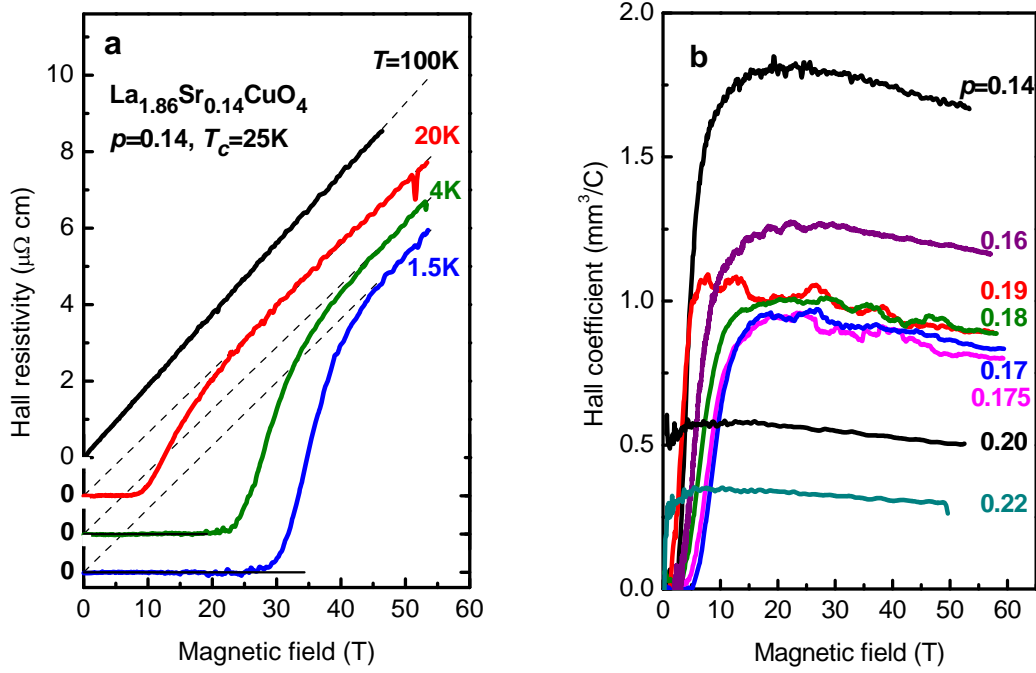


Figure 1. **(a)** In-plane Hall resistivity, ρ_{Hall} , versus magnetic field for the $\text{La}_{1.86}\text{Sr}_{0.14}\text{CuO}_4$ thin film sample. Above T_c , $\rho_{Hall}(H)$ behaves conventionally (i.e. is linear in magnetic field for all fields). Below T_c , the low noise level for these measurements enables a high-precision determination of the recovery of conventional linear-in-field normal state behavior that extrapolates through the origin (dotted lines) once superconductivity is suppressed by the magnetic field. **(b)** Hall coefficient, $R_H = \rho_{Hall}(H) / H$, as a function of magnetic field at $T=20\text{K}$ showing the non-monotonicity of R_H on doping, p . Note that the curve for $p=0.175$ lies below the curves for *both* slightly lower doping ($p=0.16$ and 0.17) and slightly higher doping ($p=0.18$ and 0.19) Sr doping. For clarity, data from several temperatures and doping levels are not plotted.

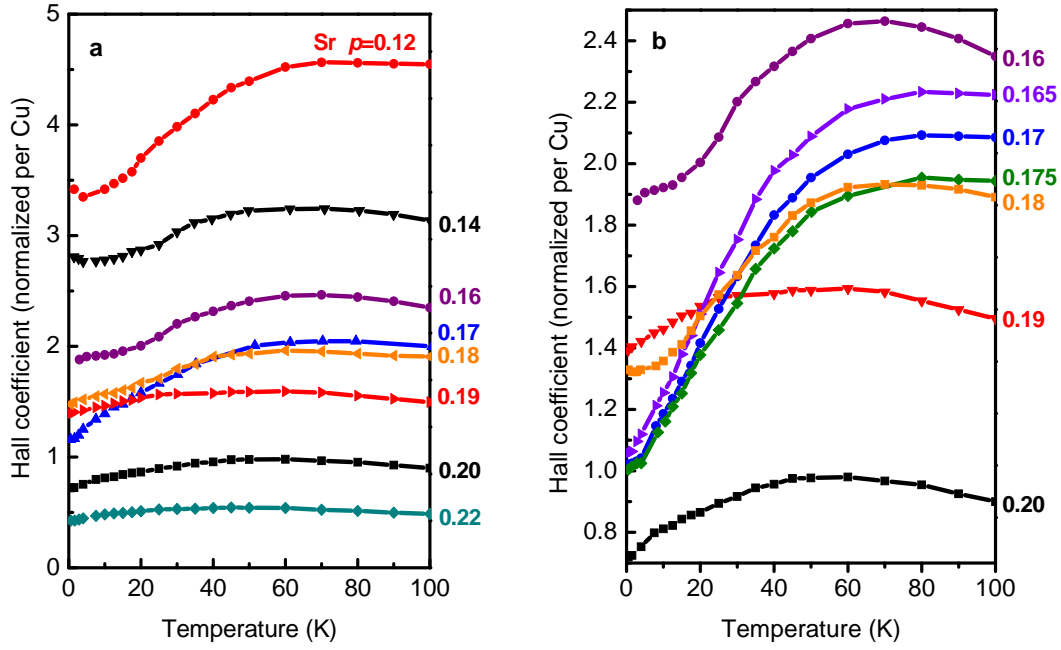


Figure 2. **(a)** Temperature dependence of the high-field Hall coefficient, R_H , normalized per Cu atom, at various doping levels $0.12 < p < 0.22$. For clarity, data from several doping levels studied are not plotted. **(b)** An expanded view of the measurements from all samples with doping levels near optimum doping. While at high temperature R_H doping dependence is monotonic, low temperature data shows a local minimum at $p=0.175$.

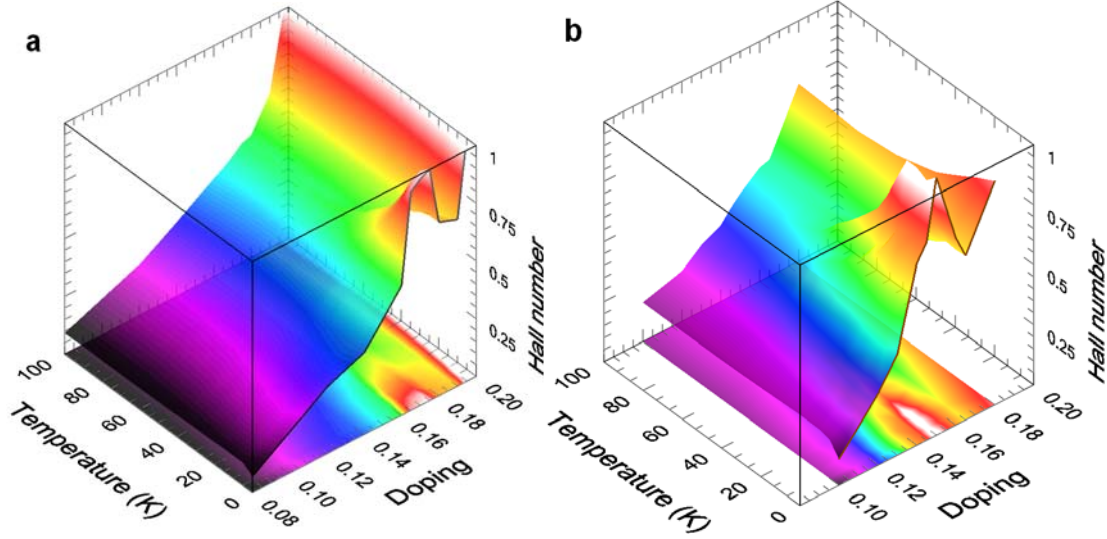


Figure 3. **(a)** Doping dependence of the p-type Hall number (defined as $1/R_H$ and normalized per Cu atom) in of $\text{La}_{2-p}\text{Sr}_p\text{CuO}_4$, in which intense magnetic fields have suppressed superconductivity. At high temperatures, we find that the Hall number remains relatively low in underdoped samples and that above $p \sim 0.17$ the Hall number increases rapidly with increasing doping. As p approaches 0.30, the Hall number diverges when the curvature of the energy band changes sign and the transport crosses from holes to electrons above $p \sim 0.30$ ^{27,28}. The most striking feature of the Hall number is the cusp at $p \sim 0.175$, which develops at low temperatures. **(b)** Hall number in platelets of $\text{Bi}_2\text{Sr}_{2-x}\text{La}_x\text{CuO}_{6+\delta}$ single crystals (adapted from ref. 6) displays a similar low-temperature peak near optimum doping.

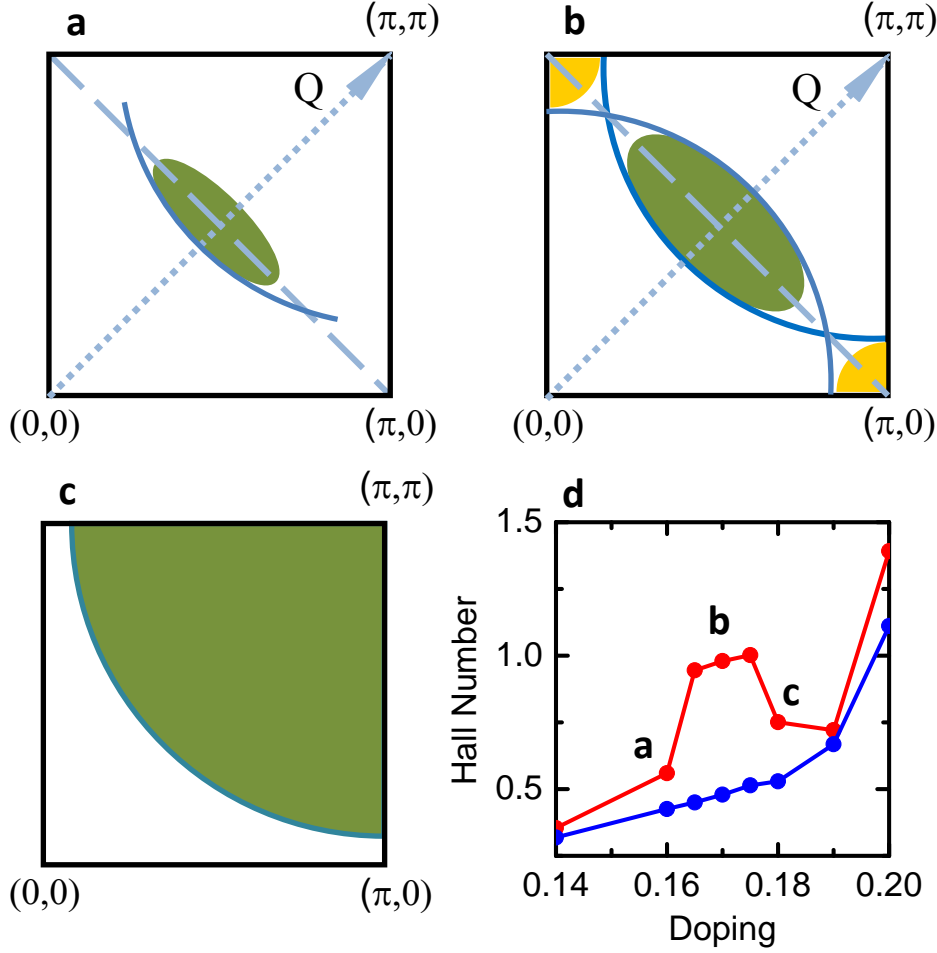


Figure 4. Schematic evolution of the Fermi surface with increasing doping from (a) to (b) to (c) shown in the first quadrant of the Brillouin zone. The two colors denote hole (dark green) and electron (yellow) pockets. Solid line in panel a indicates Fermi arc observed in ARPES measurements (see text). Dashed line indicates Brillouin zone folding that results from an order parameter with modulation vector $Q = (\pi, \pi)$ (dotted arrow) resulting in hole-like quasiparticles. We have considered the report that the SdH

oscillations are due to electron pockets²⁹, in which case it can be debated whether the hole-like states around $(\pi/2, \pi/2)$ form a classical Fermi pocket (green area on panel **a**) or an open "Fermi arc" (blue arc on panel **a**). We note that the peak in Hall number reported here would be observed in both scenarios, without changing our main conclusions. **(b)** Increased doping expands the hole pocket and the onset of the peak in the Hall number is ascribed to the emergence of electron pockets (yellow areas) near optimum doping. With further doping **(c)**, the order parameter is suppressed, which destroys the electron pocket and completes the transition to the large pocket Fermi surface. **(d)** Hall number data from Fig. 3a for $T=1.5$ K (red) and $T=100$ K (blue). Letters a, b, c denote the doping regimes corresponding to the three Fermi surface diagrams in panels **a**, **b**, and **c** respectively.

Supplementary information

Low temperature normal state of LSCO thin films

Suppression of superconductivity by high magnetic fields reveals dramatic changes in transport properties of LSCO films as a function of doping at low temperatures. Whereas the overdoped thin film samples with $p > 0.19$ remain metallic ($d\rho_{ab}/dT > 0$) to $T \sim 1.5\text{K}$, the lowest temperature measured, the underdoped and optimally doped samples display a resistivity minimum and a crossover to insulating behavior ($d\rho_{ab}/dT < 0$) at these same low temperatures. This transition from an insulating to a metallic normal state occurs for $p = 0.19$ with $\rho_{ab} \sim 0.09 \text{ m}\Omega\text{-cm}$, a resistivity value similar to one reported for single crystals of LSCO and BSLCO¹⁻³.

Non-linear Hall response

A feature evident in Fig. 1b and not mentioned in the main text is that $R_H(H)$ decreases with increasing field because $\rho_{Hall}(H)$ is slightly sub-linear. While this effect is sufficiently small that it does not change the salient conclusions of this paper, we note that the departure from linearity is larger as p increases. As recently demonstrated for an electron-doped cuprate superconductor⁴, this is most likely a precursor of the eventual change of sign of R_H at $p \sim 0.3$ ^{5,6}.

References

1. Ando, Y., Boebinger, G. S., Passner, A., Kimura, T. & Kishio, K. Logarithmic divergence of both in-plane and out-of-plane normal-state resistivities of

- superconducting $\text{La}_{2-x}\text{Sr}_x\text{CuO}_4$ in the zero-temperature limit. *Phys. Rev. Lett.* **75**, 4662-4665 (1995).
2. Boebinger, G. S. *et al.*, Insulator-to-metal crossover in the normal state of $\text{La}_{2-x}\text{Sr}_x\text{CuO}_4$ near optimum doping. *Phys. Rev. Lett.* **77**, 5417-5420 (1996).
 3. Ono, S. *et al.* Metal-to-Insulator Crossover in the Low-Temperature Normal State of $\text{Bi}_2\text{Sr}_{2-x}\text{La}_x\text{CuO}_{6+\delta}$. *Phys. Rev. Lett.* **85**, 638-641 (2000).
 4. Li, P., Balakirev, F. F. & Greene, R. L. High-field Hall resistivity and magnetoresistance of electron-doped $\text{Pr}_{2-x}\text{Ce}_x\text{CuO}_{4-\delta}$. *Phys. Rev. Lett.* **99**, 047003 (2007).
 5. Hwang, H. Y. *et al.* Scaling of the temperature dependent Hall effect in $\text{La}_{2-x}\text{Sr}_x\text{CuO}_4$. *Phys. Rev. Lett.* **72**, 2636-2639 (1994).
 6. Tsukada, I. & Ono, S. Negative Hall coefficients of heavily overdoped $\text{La}_{2-x}\text{Sr}_x\text{CuO}_4$. *Phys. Rev. B* **74**, 134508 (2006).